

## Lattice Boltzmann model for diffusion-controlled dissolution of solid structures in multicomponent liquids

F. Verhaeghe,\* S. Arnout,† B. Blanpain, and P. Wollants

Department of Metallurgy and Materials Engineering, Katholieke Universiteit Leuven, Belgium

(Received 6 April 2005; published 28 September 2005)

A lattice Boltzmann model for the dissolution of solid structures of arbitrary shape in multi-component liquids is developed. To model diffusion-controlled dissolution, a multicomponent boundary condition is presented to impose a fixed concentration on an arbitrarily located boundary. The dissolution rate of the solid is calculated based on the diffusion flow in the boundary layer. The model is validated using analytical solutions of simple dissolution problems in a static fluid, and is applied to the dissolution of a cylinder in a laminar flow.

 DOI: [10.1103/PhysRevE.72.036308](https://doi.org/10.1103/PhysRevE.72.036308)

PACS number(s): 47.10.+g, 47.11.+j, 05.20.Dd

Over the last two decades the lattice Boltzmann equation (LBE) [1–9] has evolved into a useful computational method for simulating complex flows such as multi phase [10–13] and multi component flows [14–16], flows through porous media [8], and particulate suspensions in fluid flows [17]. Dissolution of arbitrarily-shaped solid structures in multi component fluids is an application which can be quite hard to tackle with conventional techniques. For this application there is a growing interest in the lattice Boltzmann method. Kang and co-workers [18,19] developed a lattice Boltzmann model to simulate dissolution and precipitation in porous media in which they use separate populations for fluid flow and for solute transport. The assumptions made are that the solute concentration is sufficiently low so that it does not influence the flow and that the dissolution rate is limited by first order reaction kinetics. Verberg and Ladd [20] simulate diffusion-controlled dissolution using a lattice Boltzmann scheme for the fluid flow calculations, a stochastic algorithm to solve the solute concentration field, and calculate the evolution of the solid structure from the local diffusion flux.

In the present work we use the two-fluid model for binary mixtures proposed by Luo and Girimaji [21,22], in which the kinetic theory mixture model suggested by Sirovich [23] is discretized in an *a priori* fashion [5–7], yielding the following set of lattice Boltzmann equations:

$$f_{\alpha}^{\sigma}(\mathbf{x}_i + \mathbf{e}_{\alpha} \delta_i, t + \delta_t) - f_{\alpha}^{\sigma}(\mathbf{x}_i, t) = J_{\alpha}^{\sigma\sigma} + J_{\alpha}^{\sigma\varsigma} \quad (1)$$

with  $f_{\alpha}^{\sigma}$  the distribution function for component  $\sigma$  and velocity  $\mathbf{e}_{\alpha}$ . The self-collision term  $J_{\alpha}^{\sigma\sigma}$  and the cross-collision term  $J_{\alpha}^{\sigma\varsigma}$ , describing the effect of collisions of like and different particles, respectively, are given by

$$J_{\alpha}^{\sigma\sigma} = -\frac{1}{\tau_{\sigma}} [f_{\alpha}^{\sigma} - f_{\alpha}^{\sigma(0)}],$$

$$J_{\alpha}^{\sigma\varsigma} = -\frac{1}{\tau_D} \frac{\rho_{\varsigma}}{\rho} \frac{f_{\alpha}^{\sigma(eq)}}{R_{\sigma} T} (\mathbf{e}_{\alpha} - \mathbf{u}) \cdot (\mathbf{u}_{\sigma} - \mathbf{u}_{\varsigma}),$$

where  $\rho_{\sigma}$  and  $\rho_{\varsigma}$ , and  $\mathbf{u}_{\sigma}$  and  $\mathbf{u}_{\varsigma}$  are the mass densities and the flow velocities for the species  $\sigma$  and  $\varsigma$ , defined as the moments of the distribution functions:

$$\rho_{\sigma} = \sum_{\alpha} f_{\alpha}^{\sigma} = \sum_{\alpha} f_{\alpha}^{\sigma(0)}, \quad (2a)$$

$$\rho_{\sigma} \mathbf{u}_{\sigma} = \sum_{\alpha} f_{\alpha}^{\sigma} \mathbf{e}_{\alpha} = \sum_{\alpha} f_{\alpha}^{\sigma(0)} \mathbf{e}_{\alpha}. \quad (2b)$$

The equilibrium distribution function  $f_{\alpha}^{\sigma(0)}$  has the following form:

$$f_{\alpha}^{\sigma(0)} = \left[ 1 + \frac{1}{R_{\sigma} T} (\mathbf{e}_{\alpha} - \mathbf{u}) \cdot (\mathbf{u}_{\sigma} - \mathbf{u}) \right] f_{\alpha}^{\sigma(eq)},$$

$$f_{\alpha}^{\sigma(eq)} = w_{\alpha} \rho_{\sigma} \left[ 1 + \frac{\mathbf{e}_{\alpha} \cdot \mathbf{u}}{R_{\sigma} T} + \frac{(\mathbf{e}_{\alpha} \cdot \mathbf{u})^2}{2(R_{\sigma} T)^2} - \frac{\mathbf{u} \cdot \mathbf{u}}{2R_{\sigma} T} \right]$$

with the weight factors  $w_{\alpha}$  dependent on the choice of the discrete velocity set  $\mathbf{e}_{\alpha}$ .

Through the Chapman-Enskog analysis (a multiple-scale expansion) [24] the macroscopic equations solved by the model can be derived. This leads to the following convection-diffusion equation for the difference in mass fraction  $\phi = (\rho_{\sigma} - \rho_{\varsigma}) / (\rho_{\sigma} + \rho_{\varsigma}) = x_{\sigma} - x_{\varsigma}$ :

$$\partial_t \phi + \mathbf{u} \cdot \nabla \phi = \frac{1}{\rho} \nabla \cdot (D \nabla \phi + \mathbf{F}) \quad (3)$$

with  $D$  the diffusion coefficient, related to the relaxation time  $\tau_D$  and the properties of the species, and  $\mathbf{F}$  a force term including a pressure gradient dependence and external force contributions [22].

In the present work a two-dimensional model is used to study the dissolution of solid structures with an arbitrary shape and composition in a binary fluid containing species  $\sigma$  and  $\varsigma$ . The solid structure is discretized using a finite volume approach. To each calculation node a volume fraction  $a$  of solid is assigned. Cells with no solid fraction are labeled fluid cells, cells partially or fully solid are labeled solid cells. The location of a boundary between a fluid node and a neighboring solid node can be explained using Fig. 1. For every direction  $\mathbf{e}_{\alpha}$  the solid surface is taken to be at a fraction  $(\frac{3}{2} - a)$  of the lattice spacing in that direction.

We assume the dissolution to be diffusion-controlled, which means that diffusion is the rate-limiting step and the chemical reaction rate is considered very fast compared to diffusion. To simulate a diffusion-controlled dissolution

\*Electronic address: Frederik.Verhaeghe@mtm.kuleuven.be

†Electronic address: Sander.Arnout@mtm.kuleuven.be

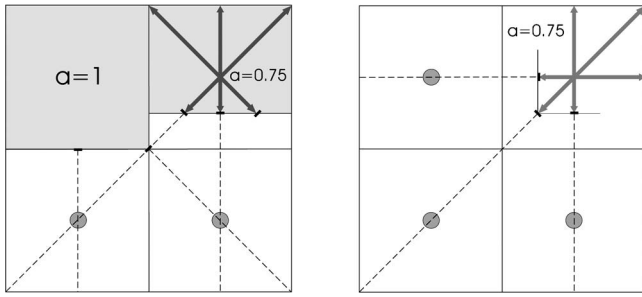


FIG. 1. Examples of boundary locations for different solid geometries. Dashed lines (- -) indicate velocity directions, dashes (-) indicate location of boundary for crossing velocity direction.

mechanism two conditions have to be imposed: an equilibrium concentration of both species on the interface between solid and liquid, and the dissolution of the solid according to the diffusion flux.

The concentration boundary condition used to impose a fixed mass fraction on the solid interface can be explained using Fig. 2. Let  $r_j$  be a fluid node with a neighboring solid node  $r_s$ . Let the velocity streaming into the wall be  $e_\alpha$  and the opposite velocity be  $e_{\bar{\alpha}}$ . After the collision step, the populations  $f_\alpha^k$  and  $f_{\bar{\alpha}}^k$  are known in the fluid nodes  $r_j, r_{j'}$ , and  $r_{j''}$ . After streaming the populations  $f_{\bar{\alpha}}^k$  are not known in  $r_j$  and have to be calculated from the boundary condition. If the solid node  $r_s$  is completely filled with solid, that is if  $a=1$ , we have found that the following expression can be used to calculate the  $f_{\bar{\alpha}}^k$  populations for both components from the known populations  $f_\alpha^k$ :

$$f_{\bar{\alpha}}^\sigma = 2x_\sigma(f_\alpha^\sigma + f_\alpha^\xi) - f_\alpha^\sigma \quad (4)$$

in which  $x_\sigma$  is the imposed equilibrium mass fraction of component  $\sigma$  on the solid surface. The rationale behind this

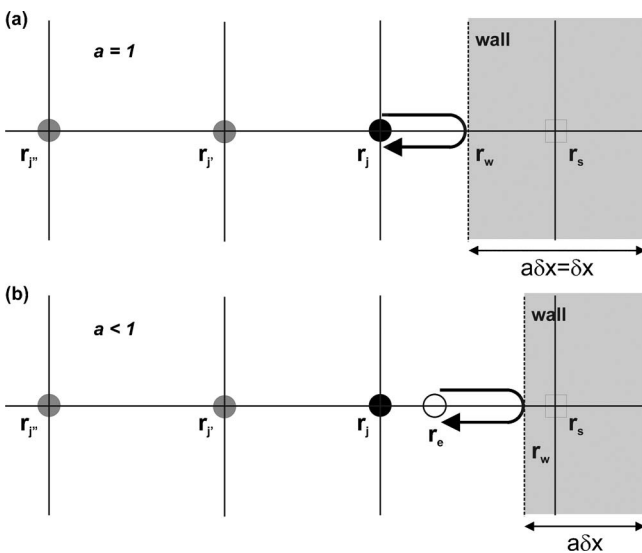


FIG. 2. Illustration of the boundary condition. Shaded disks are fluid nodes, with the disks (•) fluid nodes with a solid neighbor node. Circles (○) are located in the fluid but not on grid nodes. Square boxes indicate solid nodes.

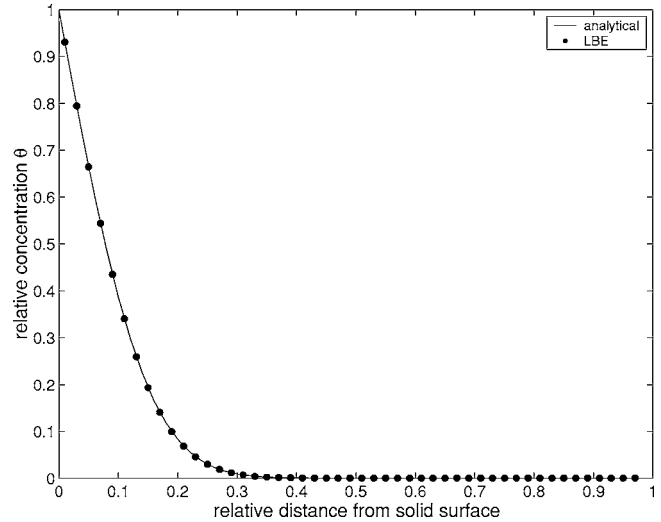


FIG. 3. Validation of static LBE calculation with analytical results.

boundary condition expression can be seen by rewriting it in the following way:

$$f_\alpha^\sigma + f_{\bar{\alpha}}^\sigma = 2x_\sigma(f_\alpha^\sigma + f_\alpha^\xi) \approx 2x_\sigma w_i \rho \approx 2w_i \rho_\sigma. \quad (5)$$

In simple terms this means that the mass of  $\sigma$  moving along the directions  $\alpha$  and  $\bar{\alpha}$  is set equal to twice the mass of  $\sigma$  moving along  $\alpha$ , calculated from both species populations and the imposed mass fraction on the solid interface.

Since in general the boundary will not be located half way, a procedure of interpolation and extrapolation has been developed which can be explained using Fig. 2(b). If  $a < 1$ , a fictitious node can be created half a lattice spacing from the boundary. For this node the populations  $f_{\bar{\alpha}}^k$  can be calculated using relation (4) if the populations  $f_\alpha^k$  are known. These can be calculated from extrapolation using the values in the nodes  $r_j, r_{j'}$ , and  $r_{j''}$ . From the calculated population  $f_{\bar{\alpha}}^k$  in the fictitious node, and the populations  $f_\alpha^k$  known in  $r_{j'}$  and  $r_{j''}$

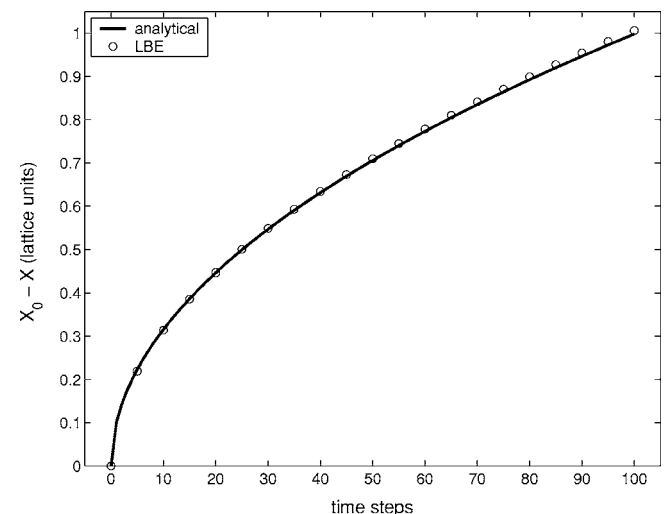


FIG. 4. Validation of moving boundary condition with analytical results.

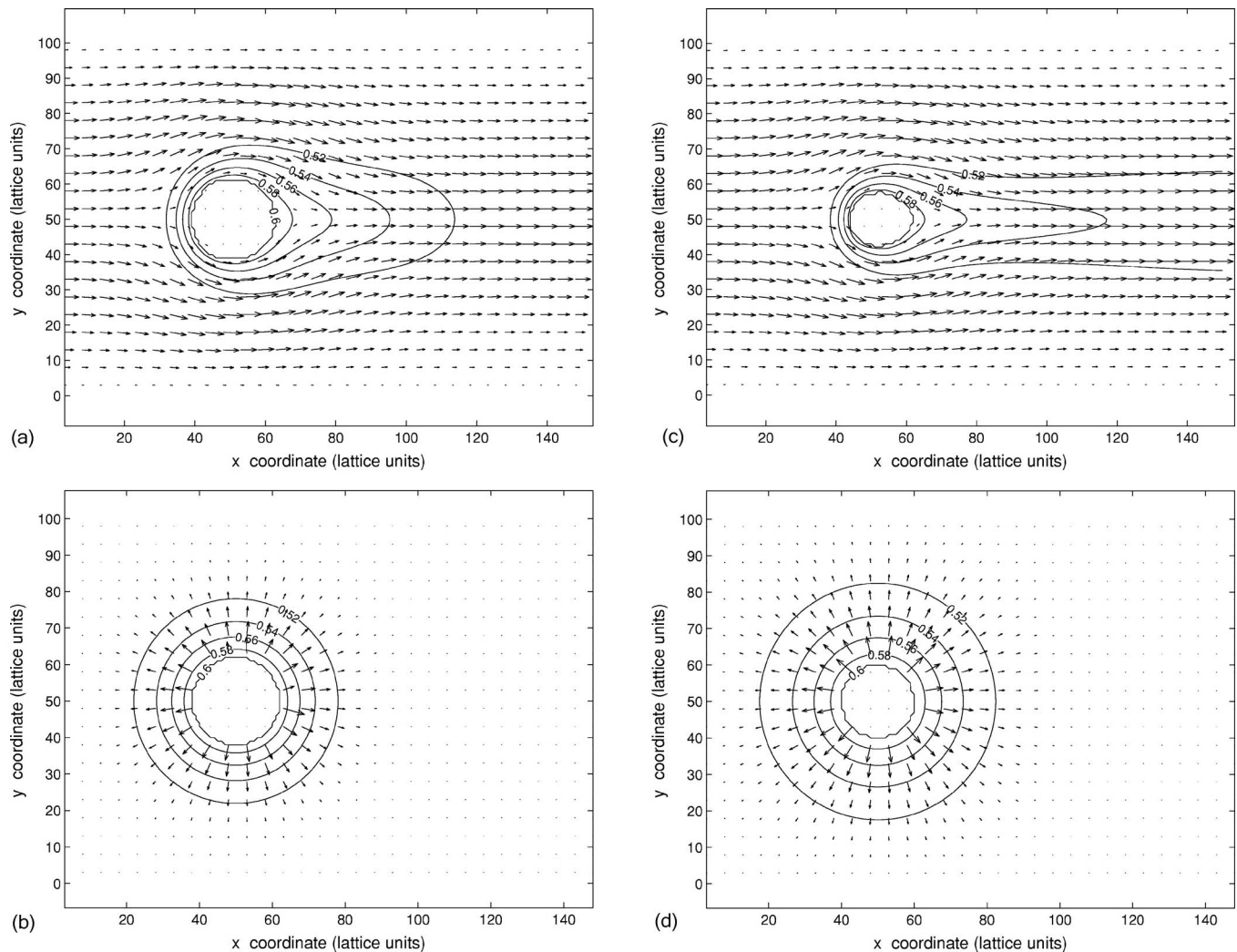


FIG. 5. Simulated concentration profiles and velocity fields for a cylinder with and without flow. (a) and (c) show the resulting structure with convection after two different times. Contours indicate the concentration profile, arrows the flow field. (b) and (d) show the resulting structure without convection after two different times. Contours indicate the concentration profile, arrows indicate the diffusive flux field.

(through simple streaming), the populations  $f_{\alpha}^k$  in  $r_j$  can be interpolated.

Once the concentration boundary condition has been imposed on all nodes with neighboring solid nodes, the amount of dissolving solid can be calculated. For each solid node surrounded by at least one fluid node, the diffusing amount of a component can be calculated by summing the difference in mass of that component before and after application of the boundary condition for all fluid nodes surrounding the solid node under study. The mass fraction  $a$  of that node can be updated accordingly:

$$a(t+1) = a(t) - \frac{1}{(\rho_{\sigma}^S - \rho_{\sigma}^L)} \sum_{nb} (f_{\alpha}^{\sigma} - f_{\alpha}^{\sigma'}) \quad (6)$$

in which  $\rho_{\sigma}^S$  and  $\rho_{\sigma}^L$  are the density concentrations of component  $\sigma$  in the solid and in the liquid in equilibrium with the solid, respectively. The summation is made over all neighboring fluid nodes.

The proposed boundary condition has been tested for the static problem of diffusion into a semi-infinite fluid. This amounts to solving the diffusion equation:

$$\partial_t c(x,t) = D \nabla^2 c(x,t) \quad (7)$$

with initial and boundary conditions:

$$c(x,0) = c_0, \quad c(0,t) = c_1, \quad c(\infty,t) = c_0 \quad (8)$$

in which  $c_0$  and  $c_1$  are the initial concentration and the concentration at the boundary, respectively.

This can be solved analytically yielding the following concentration profile [25]:

$$\theta = 1 - \operatorname{erf}\left(\frac{x}{\sqrt{4Dt}}\right) \quad (9)$$

with  $\theta = (c - c_0)/(c_1 - c_0)$  the reduced concentration. In Fig. 3 the result of the LBE calculation is compared with the analytical result. The agreement is satisfactory.

A flat solid interface moving by diffusion is one of the few moving boundary problems with an analytical solution.

The boundary condition at  $x=0$  in Eq. (8) has to be replaced with the Stefan condition

$$(D \nabla c)_{x=X} = (1 - c_1) \frac{dX}{dt} \quad (10)$$

with  $X(t)$  the location of the interface at a given time  $t$ . The solution for  $X$  is given by [26]

$$X_0 - X = L\sqrt{Dt} \quad (11)$$

with  $X_0$  the initial position of the interface, and  $L$  a constant given by

$$\frac{C_1}{1 - C_1} = \frac{\sqrt{\pi}}{2} L \exp\left(\frac{L^2}{4}\right) \left[ 1 + \operatorname{erf}\left(\frac{L}{2}\right) \right]. \quad (12)$$

Figure 4 shows a comparison between the LBE result and the analytical solution.

To show the potentiality of the presented model the dissolution of a cylindrical solid component with and without convection in the fluid has been simulated. On a domain of  $100 \times 150$  nodes, a solid cylinder with a diameter of 26 lattice units (l.u.) and a composition of  $0.1\sigma$  and  $0.9\varsigma$  (dimensionless lattice density) is initialized. The cylinder is in equilibrium with a fluid of 60%  $\varsigma$ . The initial composition of the fluid is 50%  $\varsigma$ . In one case the fluid is static. On the domain boundaries zero velocity and zero concentration gradient is imposed. In the other case a fluid with a composition of 50%  $\varsigma$  is injected at the left-hand side of the domain. A pressure drop of  $0.01p_0$  is applied over the domain, with  $p_0$  the pressure related to dimensionless density 1. At the right-hand side a no-diffusion condition is imposed. On the upper and lower wall zero velocity and zero flux is imposed. The viscosity and diffusion coefficient are chosen so that a Schmidt number  $Sc = \nu/D = 30$  is obtained. The Reynolds number for

flow over the cylinder is about 0.5 at the start of the dissolution. Figure 5 shows the evolution of the density of  $\varsigma$  for both cases. The velocity of the fluid or the diffusion flux of  $\varsigma$  is indicated by the arrows.

Figure 5 clearly shows the off-grid nature of the boundary condition with solid fractions and extrapolation (i.e., the boundary can be arbitrarily located between grid nodes). Since the partially solid cells have the composition of the solid (so a concentration of 90%  $\varsigma$ ) in these figures, the 60%  $\varsigma$  contour shows the discretization of the solid by the lattice. However, the other contours are smooth and in the case without convection, they behave like the solid is a perfect cylinder, as can be noticed in Figs. 5(b)–5(d). In the case with convection [Figs. 5(a)–5(c)], the solid dissolves faster on the front and the sides than on the back, and a more “aerodynamic” shape evolves. The remaining amount of solid is smaller than in the case without convection.

A lattice Boltzmann model for dissolution of arbitrarily shaped solids in a multi-component liquid has been presented. The model has been validated for problems with analytical solutions. The use of the two-fluid model removes the low-concentration condition often used in previous work. The model has been applied to more complex problems such as the dissolution of a cylinder under convection. Future research may include analytical proof of the boundary condition, inclusion of temperature dependence, and extending the fluid model to multiple phases.

F.V. would like to acknowledge the support of the Research Foundation - Flanders (FWO - Vlaanderen). This research is partially funded by the IWT (Institute for Science and Technology) Project No. 030880. The authors would also like to thank Professor Jan Franssaer and Professor Li-Shi Luo for many insightful discussions.

- 
- [1] G. R. McNamara and G. Zanetti, *Phys. Rev. Lett.* **61**, 2332 (1988).
- [2] Y. Qian, D. D’Humières, and P. Lallemand, *Europhys. Lett.* **17**, 479 (1992).
- [3] H. Chen, S. Chen, and W. Matthaeus, *Phys. Rev. A* **45**, R5339 (1992).
- [4] D. D’Humières, in *AIAA Rarefied Gas Dynamics: Theory and Simulations*, Vol. 59 of Progress in Astronautics and Aeronautics, edited by B. D. Shizgal and D. P. Weaver (AIAA, Washington, DC, 1992).
- [5] X. He and L.-S. Luo, *Phys. Rev. E* **55**, R6333 (1997).
- [6] X. He and L.-S. Luo, *Phys. Rev. E* **56**, 6811 (1997).
- [7] X. Shan and X. He, *Phys. Rev. Lett.* **80**, 65 (1998).
- [8] S. Chen and G. Doolen, *Annu. Rev. Fluid Mech.* **30**, 329 (1998).
- [9] D. Wolf-Gladrow, *Lattice-Gas Cellular Automata and Lattice Boltzmann Models*, Vol. 1725 of Lecture Notes in Mathematics (Springer-Verlag, Berlin, 2000).
- [10] X. Shan and H. Chen, *Phys. Rev. E* **47**, 1815 (1993).
- [11] X. Shan and H. Chen, *Phys. Rev. E* **49**, 2941 (1994).
- [12] L.-S. Luo, *Phys. Rev. Lett.* **81**, 1618 (1998).
- [13] L.-S. Luo, *Phys. Rev. E* **62**, 4982 (2000).
- [14] X. Shan and G. D. Doolen, *J. Stat. Phys.* **81**, 379 (1995).
- [15] X. Shan and G. Doolen, *Phys. Rev. E* **54**, 3614 (1996).
- [16] M. R. Swift, E. Orlandini, W. R. Osborn, and J. M. Yeomans, *Phys. Rev. E* **54**, 5041 (1996).
- [17] D. Qi, *J. Fluid Mech.* **385**, 43 (1999).
- [18] Q. Kang, D. Zhang, and S. Chen, *Phys. Rev. E* **65**, 036318 (2002).
- [19] Q. Kang, D. Zhang, and S. Chen, *J. Geophys. Res.* **108**, 9 (2003).
- [20] R. Verberg and A. J. C. Ladd, *Phys. Rev. E* **65**, 056311 (2002).
- [21] L.-S. Luo and S. S. Girimaji, *Phys. Rev. E* **66**, 035301(R) (2002).
- [22] L.-S. Luo and S. S. Girimaji, *Phys. Rev. E* **67**, 036302 (2003).
- [23] L. Sirovich, *Phys. Fluids* **5**, 908 (1962).
- [24] S. Chapman and T. Cowling, *The Mathematical Theory of Non-Uniform Gases* (Cambridge University Press, Cambridge, England, 1970), 3rd ed.
- [25] R. B. Bird, W. E. Stewart, and E. N. Lightfoot, *Transport Phenomena* (Wiley, New York, 2002), 2nd ed.
- [26] H. B. Aaron, D. Fainstein, and G. R. Kotler, *J. Appl. Phys.* **41**, 4404 (1970).